INTERACTION OF A SHOCK WAVE WITH A RIGHT ANGLED BEND IN TWO-PHASE FLOW

K. A. IBRAHIM*

ABSTRACT :

This paper describes the prediction of the unsteady, gas-solid suspension, flow field resulting from the interaction of a shock wave with a right angled bend in two-dimensional cartesian or axisymmetric cylindrical coordinates. The finite-difference computational technique, which has been applied; by previous investigators; to the unsteady flow of a single phase compressible media, has been modified here to be applied to the analysis of suspension flow. In the development of the numerical technique, the solid phase properties are assumed to be continuous fields, since the investigation is not concerned with the behaviour of individual particles. Interaction between the phases are incorporated into the equations for the changes in the properties of the material occupying the cells. The solid particles were found to have a significant effect on the behaviour of shock wave interaction with a 90° bend in a shock tube. The results, for gas phase, were checked against the experimental results, obtained by previous investigators, and a good agreement has been obtained.

1. INTRODUCTION:

Unlike the case of single phase flow, no experimental work has been published and no analysis made of interaction of a shock wave with bends in a gas - solid suspension flow shock tube. Very little has been published concerned with theoretical studies of the flow of gas-solid suspension around solid bodies, [1-3]. Considering shock waves attached to a wedge in a two phase flow and the problem of supersonic flow of a gas containing particles past a wedge is considered, in some recent papers, by Probstein and Fassio [4], Peddieson and Lyu [5], Waldman and Reinecke [6], Spurk and Gerber [7] and Morgenthaler [8].

Problems involving the behaviour of interaction of shock waves with bends in the previous work are studied in the case of air flow only. Hence the following literature survey is concerned with the behaviour of interaction shock waves with bends in air flow only. The study of pure gas shock wave

* Sen. Lecturer, Mech. Eng. Dept., Elmonofia Univ.

interaction with corners has formed the main part of the gas dynamic research programme in the school of mechanical engineering for some years ,[9 - 16]. The unsteady, two-dimensional flow field resulting from the interaction of a moving planar shock wave with a compression corner is determined by Kutler and Shankar [9] . Their results of the numerical simulation were qualitatively very similar to the experimental results obtained by previous investigators. Experimentalists [10],[11] and theoreticians[12 - 16] have been studying the problem of shock wave diffraction, that is, the deflection of a shock wave whose normal path has been impeded by some obstacle. Skews [17] described, in his experimental study, a two dimensional interaction of shock waves having Mach numbers of 1.5 , 2.0 and 2.5 with 60 , 90 and 120 degree bends in a rectangular duct. The influence of the wall angle and shock Mach number were investigated photographically. He described also the behaviour of the reflected wave.

In spite of the above previous work, the phenomena associated with the interaction of a shock wave in gas - solid suspension flow is not well understood. All the previous work was concerned with air flow only or two - phase flow around solid bodies . Virtually no work has previously been published which considers the effect of solid particles on the behaviour of interaction of shock waves with bends. Thus this paper will describe, theoretically, the effect of solid powders on the behaviour of interaction shock waves with a 90° bend in a shock tube.

Nomenclature:

a_m = Mixture speed of sound.
c_D = Particle drag coefficient.
c_p, c_v = Specific heats of gas phase at constant pressure and at constant volume.
c_s = Solids specific heat
d = Particle diameter.
I = Specific internal energy.
ib = Coordinate subscript of corner cell.
j = Coordinate subscript in r-direction.
J = Particle temperature lag.
jb = Coordinate subscript of corner cell.
K = Particle velocity lag.
K_g = Thermal conductivity of gas phase
m = mm-1 (see Fig 1)
mm = Maximum coordinate subscript in r-direction.

M_s = Shock Mach number.
n = nn-1 (see Fig 1).
nn = Maximum coordinate subscript in z-direction.
P = Thermodynamic pressure.
r = Radial coordinate
R = Gas constant
Re = Particle Reynolds number.
S = Area, Eqs. (16 and 17).
t = Time
T_g = Gas temperature.
T_o = Stagnation temperature.
T_p = Particle temperature .
u = Resultant gas velocity $= \sqrt{u_z^2 + u_r^2}$
v = Resultant solids velocity $= \sqrt{v_z^2 + v_r^2}$
Vol = Cell volume
X = Solids loading ratio (weight of solids/weight of air).
Y = $1 - \epsilon$
Z = Axial coordinate.
ϵ = Particle phase volume fraction.
ρ = Gas density.
ρ_p = Particle material density.
σ = Mass of particles per unit volume of mixture.
δ = Particle to gas specific heat = c_s/c_p
δ_r = Cell dimension (see Fig (2 , 3)).
δ_z = Cell dimension (see Fig (2 , 3)).
ν = Kinematic viscosity.
γ = Ratio of gas specific heats = c_p/c_v.

Subscripts:

x : Initial condition behind shock wave.
y : Initial conditions ahead of shock wave.

2. Assumptions and Basic Equations:

The following assumptions will prevail throughout:

(1) The motion is two-dimensional and unsteady.
(2) The gas follows the perfect gas laws, with constant specific heats.
(3) The particles are spherical, smooth, and of constant density and specific heat.
(4) Viscous fraction and heat transfer due to the velocity and temperature gradients in the direction of the flow are neglected. The only viscous effect is the heat transfer between the phases by convection.

(5) There is no mass transfer between the flow and its surroundings or between the two phases.
(6) The particles do not interact with each other, and their shape does not change during flight.
(7) Gravity and other body forces are negligible.

In a non-equilibrium gas-solid flow there always exists a certain degree of lag between the gas and the particles, which can be expressed in the form of particle velocity and temperature lag parameters K,J respectively, where;

$$K = v/u \tag{1}$$

and

$$J = (T_o - T_p)/(T_o - T_g) \tag{2}$$

The conditions of the gas phase at each instant(t) and position (z & r) are described by resultant gas velocity u and any two of the state variables P, ρ, T_g and a_m. The particles are characterized by V, T_p and σ. The basic equations governing the flow are as follows:

Continuity equations

$$\frac{\partial \rho}{\partial t} + \frac{\partial}{\partial z}(\rho Y u_z) + \frac{\partial}{\partial r}(\rho Y u_r) = 0 \tag{3}$$

$$\frac{\partial \sigma}{\partial t} + \frac{\partial}{\partial z}(\sigma v_z) + \frac{\partial}{\partial r}(\sigma v_r) = 0 \tag{4}$$

Overall momentum equations:

$$\frac{\partial}{\partial t}(\rho Y u_z + \sigma v_z) + \frac{\partial}{\partial z}(\rho Y u_z^2 + \sigma v_z^2) + \frac{\partial P}{\partial z} = 0 \tag{5}$$

$$\frac{\partial}{\partial t}(\rho Y u_r + \sigma v_r) + \frac{\partial}{\partial r}(\rho Y u_r^2 + \sigma v_r^2) + \frac{\partial P}{\partial r} = 0 \tag{6}$$

Overall energy equations

$$\frac{\partial}{\partial t}\left[\rho(c_v T_g + \tfrac{1}{2}u_z^2)Y + \sigma(c_s T_p + \tfrac{1}{2}v_z^2)\right] + \frac{\partial}{\partial z}\left[\rho u_z(c_p T_g + \tfrac{1}{2}u_z^2)Y + \sigma v_z(c_s T_p + \tfrac{1}{2}v_z^2)\right] = 0 \tag{7}$$

$$\frac{\partial}{\partial t}\left[\rho(c_v T_g + \tfrac{1}{2}u_r^2)Y + \sigma(c_s T_p + \tfrac{1}{2}v_r^2)\right] + \frac{\partial}{\partial r}\left[\rho u_r(c_p T_g + \tfrac{1}{2}u_r^2)Y + \sigma v_r(c_s T_p + \tfrac{1}{2}v_r^2)\right] = 0 \tag{8}$$

Equation of state

$$P = (\gamma - 1)\rho I \tag{9}$$

Phase interactions:

Regardless of the mathematical model used to represent the suspension flow, its applicability obviously depends on the correct representation of the laws governing the exchange of momentum and energy between the phases. The equation of motion for the particle can be written as in [21] ;

$$\frac{\partial v}{\partial t} + v\left(\frac{\partial v}{\partial z} + \frac{\partial v}{\partial r}\right) = \frac{3}{4} \cdot \frac{1}{\rho_p d} \cdot C_D \cdot \rho \cdot (u-v)\,|u-v| \qquad (10)$$

In the present investigation, an approximation to the standard drag curve ($C_D \propto Re$) for a sphere was adopted as in [18] as follows.

$$\left.\begin{aligned} C_D &= 24/Re && \text{for } Re < 0.1 \\ C_D &= (24 + 0.379 Re^{0.66})/Re && 0.1 < Re < 500 \\ C_D &= 2.63/Re^{0.26} && 500 < Re < 1000 \\ C_D &= 0.44 && Re > 1000 \end{aligned}\right\} \qquad (11)$$

The particle Reynolds number, Re, is defined as

$$Re = |u - v| \cdot d/\nu \qquad (12)$$

Heat transfer effects are represented by formulas which give the dependence of the Nusselt number, Nu, on the particle Reynolds number and the Prandtl number, P_r , of the gas, [18] .

$$Nu = 2 + 0.459\ Re^{0.55} \cdot P_r^{0.33} \qquad (13)$$

The Prandtl number was assumed to be 0.7 over the expected temperature range as in [18] .With assumptions analogous to those for the particle motion, the heat balance between the gas and the particles is given ,as in [21] , by:

$$\frac{\partial T_p}{\partial t} + V\left(\frac{\partial T_p}{\partial z} + \frac{\partial T_p}{\partial r}\right) = \frac{6 K_g}{\rho_p d^2} \cdot \frac{Nu}{C_s} (T_g - T_p) \qquad (14)$$

3. Computational technique

The finite-difference computational technique used, to solve the governing equations (1) through (14), is that described, for gas phase, by Gentry, et al. [19] . This technique, which has been developed here for use in suspension flow, known as the Fluid-in-cell(FLIC) method.

3.1: The computational procedure

The computational method (FLIC) may be drawn as follows:

1. The flow field is divided into a number of regions or cells which are fixed in space.
2. The material contained within a cell, both gas and solid particles, is represented by a discrete number of separate gas and solid mass points.
3. The velocity of all the gas and solid mass points in any cell is calculated after a time interval using the equation of motion. This equation includes the interactive force between the phases.
4. The energy equation, which also includes phase interaction terms, is used to determine the internal energy of the gas and solid at the end of the time step.
5. The total momentum and total energy of each phase are then calculated.
6. A weighted average velocity for each mass points (gas & solid) is obtained taking into account the velocities in the neighbouring cell and the distance from the cell boundary. The distance travelled by each mass point during the calculation time step is then determined.
7. The new location of all gas and solid mass points are examined to see whether they have crossed over to a new cell.
8. The mass, monentum and energy of each cell are now re-calculated and new average mass point velocities determined on the basis of the new total mass and total momentum.
9. The process is repeated.

3.2: The computing mesh.

The computing mesh is calculated by the numerical technique as follows :
nn and mm give the size of the mesh, including the boundary cells, while ib and jb are the coordinates of the corner cell, Fig.(1). When allowance is made for the boundary cells it is easily seen that the two legs of the duct are (jb - 2) and (nn - ib - 1) cells wide. The actual sizes can be found by multiplying these widths by the cell dimensions.

Fig(1) shows also the boundary conditions, where boundary 5 and 6 indicate open (continuative output) or closed (reflective) boundaries, respectively .

Boundary 3 is always considered to be open and boundaries 1,2 and 4 closed. In the calculation the cell is chosen to be in cylindrical or cartesian coordinates. For the cartesian case each cell of the mesh is a right parallelepiped with dimensions ($\delta_r \times \delta_z$) and of unit depth, Fig.(2). In cylindrical coordinates , Fig.(3), each cell is a torus of rectangular section with inner and outer radii $(j - 2)\,\delta_r$ and $(j - 1)\,\delta_r$, respectively, and width δ_z. The volume of the cell is then given by.

$$Vol_j = 2\pi\delta_r^2 \cdot \delta_z \cdot (j - 1.5) \qquad (15)$$

and the area of contact between cells (i,j) and(i+1,j) is :

$$S_j^z = 2\pi\delta_r^2 \cdot (j - 1.5) \qquad (16)$$

The average of the areas of contact between cell (i,j) and cells (i,j-1) and (i,j+1) is

$$S_j^r = 2\pi\delta_r \cdot \delta_z \cdot (j - 1.5) \qquad (17)$$

3.3: Initial Flow Conditions :

The flowfield is initialised so that the shock wave is situated at the corner (between cells ia and ib), Fig.(1). The input to the numerical calculation has been chosen to correspond closely with accepted experimental parameters. This input consists of the ambient pressure and temperature, and the shock Mach number (P_y , T_y, M_s). Also required are the physical characteristics of gas and solid particles. According to Mobbs, et al. [20] , the following relationships are apply ;

Pressure ratio across the shock

$$\frac{P_x}{P_y} = \frac{2N}{N+1} M_s^2 - \frac{N-1}{N+1}$$

Density ratio across the shock

$$\frac{\rho_x}{\rho_y} = \frac{(N+1)\,M_s^2}{2 + (N-1)\,M_s^2}$$

Temperature ratio across the shock

$$\frac{T_{gx}}{T_{gy}} = \left(\frac{2NM_s^2 - (N-1)}{N+1}\right)\left(\frac{2+(N-1)\,M_s^2}{(N+1)\,M_s^2}\right)$$

Velocity ratio across the shock

$$\frac{u_x}{u_y} = \frac{2 + (N-1)M_s^2}{(N + 1)M_s^2}$$

Where, N is the index of expansion when the proportion of solids by volume is not small (i.e. solids volume is considered)

$$N = \frac{E}{E - F}$$

where,

$$E = 1 + (1 + X J \delta) / (\gamma - 1)$$

$$\delta = C_s/C_p$$

$$F = \frac{(1 + X K^2)(1 + \epsilon)}{1 + X K} - K\epsilon$$

The mixture speed of sound is obtained by [20] as follows;

$$a_m^2 = (1 + \epsilon)^2 \cdot \left(\frac{NR T_g}{1 + X K}\right)^2$$

4. Results and Discussion:

Fig (4) shows the shape of a Mach 1.5 shock wave 100 μs after it leaves the open end of a cylindrical shock tube, for pure air flow calculations. While Fig. (5) shows a result for a suspension flow parameters, X = 1.0 and polystyrene powder of 100 microns particle diameter.

Fig.(6) shows the pressure history 25 mm down - stream of the mouth of the shock tube, on the axis of symmetry for the first 150 μs of the problem time . The results are for pure air (X = 0.0) and suspension flow with different values of solids loading ratios , X. The results are corresponding to 100 μ particle diameter suspended in air. In Figs(4 , 5 and 6) the shock tube diameter was 100 mm , the mesh was chosen to be 40 x 40 cells and boundaries 5 and 6, Fig.(1), were considered to be open. The cell is chosen to be in cylindrical coordinates, Fig (3), with dimensions calculated through the computer programme, δ_r was found to be 3.57×10^{-3} m. (for jb = 16) and δ_z is calculated so that the point where the pressure history is required lies in the centre of a cell. The ambient pressure and the absolute gas temperature are 0.82×10^5 N/m^2 and 293°k, respectively. The values of velocity lag k and particle thermal lag J were chosen to be 0.98 and 0.95, respectively.

From Fig.(6) it can be seen that, the pressure decreases, especially when the proplem time increases, as the solids loading ratio increases. This is due to frictional effects throughout the flow and to the pressnce of solid particles providing an additional pressure drop component through the mechanism of momentum exchange between the two phases and the additional turbulent energy produced in the flow. The combination of these effects causes the value of pressure to be lowered as the solids loading ratio is increased.

Fig.(7) indicates the variation of the gas and particle temperature, at 25 mm down-stream of the mouth of the shock tube, against the problem time. The results are for the suspension flow conditions like that in Fig (6). From these curves it can be seen that, the gas temperature is greater than the solid temperature and the solid temperature increases. The behaviour of the gas temperature ,T_g, is particularly interesting The gas temperature rises until it reaches its peak value, followed by a less rapid decline, This is because, the velocity lag (K) is large and the effect of exchange of momentum is predominant. As (K) becomes progressively smaller the heat transfer increases in importance and eventually becomes the dominant factor and the gas temperature starts to fall again.

Fig.(8) shows the behaviour of the resultant gas and particle velocities, at 25 mm downstream of the mouth of the shock tube, after the shock wave interaction with a 90° bend, through the first 150 μ s of the problem time. The initial conditions for the suspension flow parameters are like that in Fig (6). In all these curves the resultant gas velocity (u) is greater than the resultant particle velocity (v),while both of u and v are decreases with the increase of the amount of solids in the mixture. These results can be explained as being due to an increase in the solids loading ratio causing an increase in the number of particles in a given volume of gas with a consequent rise in total drag and heat transfer rate. The increased effect of drag and heat transfer causes a decrease in flow properties.

In order to check the accuracy of the computational technique used in this paper, the results were checked against the experimental results obtained by other investigators, for pure air flow only. Fig.(9) compares pressure readings taken at a point 26 mm downstream of the corner (on the centre line of the upstream leg) with the computed solution for a Mach 1.5 shock wave. The results show a good a greement with the experimental data, obtained by Skews [17], of shock wave interaction with a right angled bend in a square tube 44 mm wide. Fig (9) also shows the variation of pressure for the suspension flow in this square tube. Unfortunately no experimental results for suspension flow have been published. Therefore, in order to check these results with the experimental ones, an experimental investigation based on the interaction of shock waves with bends in gas-solid suspension flow is suggested to carry out in the future work.

5. Conclusion:

A two-dimensional approximation to unsteady non-equilibrium gas-solid flow in a shock tube has been shown to produce solutions which give a reasonably accurate prediction of the shock wave interaction with a 90° bend in a real gas-solid flow. The general flow equations for gas-solid suspension flow along the shock tube were derived. The equations are formulated in the absence of the common assumptions of neglecting the solids volume and assuming equilibrium conditions prior to the shock. An analysis based on the Fluid in cell method was used in the computational technique. The results of the numberical method were shown to agree well with that experimentally obtained by previous investigators for the gas phase. The numerical method was discussed for both cases of cylindrical and cartesian coordinates. The variation of flow properties, pressure, gas velocity, gas temperature, solid velocity and solid temperature has been shown to depend significantly on the presence of solid particles in the air flow, and also on the amount of these particles in the mixture.

References :

1. Sone, Y., " Flow of dusty gas past a body " J. of Phy. Soc. of Japan, Vol. 33, P. 242, 1972.

2. Miura, H., " Supersonic flow of a dusty gas over a slender wedge " J. of Phy. Soc. of Japan, Vol. 37, No.2, P. 497, 1974.

3. Miura, H., " Supersonic flow of a lightly dust - Landen gas past a wedge ", J. of Phy.Soc. of Japan, Vol. 38, No. 1, P. 252., 1975.

4. Probstein, R.F. and Fassio, F., " Dusty hypersonic flows " AIAA J., Vol. 8, No.4, P. 772., 1970.

5. Peddieson Jr., J. and Lyu, C.H., " Dusty hypersonic wedge flow", AIAA J., Vol. 11, No.1, P. 110, 1973.

6. Waldman, G.D. and Reinecke, W.G., " Particle trajectories, heating and breakup in hypersonic shock layers ", AIAA J., Vol. 9, P. 1040, 1971.

7. Spurk, J.H. and Gerber, N. " Dust collection efficiency for power law bodies in hypersonic flight ", AIAA J., Vol. 10, P. 755, 1972.

8. Morgenthaler , J.H., " Analysis of two-phase flow in supersonic exhausts", Detonation and two-phase flow., Progress in Astronoutics and Rocketry, Vol. 6, P. 145, 1962.

9. Kutler, P. and Shankar, V., " Diffraction of a shock wave by a compression corner : I. Regular Reflection" AIAA J., Vol. 15 No.2, P. 197, 1977.

10. Bertrand , B.P., Measurement of pressure in Mach reflection of strong shock waves in a shock tube", Ballistic Research labs, Aberdeen , Proving Ground, Md., Memorandum Rept.2196, June 1972.

11. Bazhenova, T.V., Gvozdeva,L.G., Komarov,V.S., and Sukhov,B.G., " Diffraction of strong shock waves by convex corners" Izvestiya Akademii Nauk SSSR. Mekhanika Zhidkostii Gaza, No. 4 July-Aug., PP. 122-134, 1973.

12. Pack, D.C. " The reflection and diffraction of shock waves" J. of Fluid Mech. Vol.18, P.549,1964.

13. Rusanov, V.V., " Calculation of the interaction of Non-stationary shock waves and obstructions", J.of numerical Analysis and Mathematical Phys., Vol. 1, P. 267, 1961.

14. Zumwalt, G.W., " Weak wave Reflections at Near 90° angle of incidence" J. of applied Mechanics, P.1142, 1974.

15. Zhigalko, Y.F., " Approximate locally Non-linear solution of the problem on Interaction between a shock wave and Rigid wall", Fluid Mech.-Soviet Research, Vol. 4, P. 81, 1975.

16. Shankar, V.S.V., Kutler, P., and Anderson,D.A., " Diffraction of a shock wave by a compression corner, part II single Mach reflection", AIAA paper 77-89 , Los Angeles, Calif., 1977.

17. Skews, B.W., " Experimental study of the interaction of shock waves with bends in a duct ", Symposium on internal flows, university of salford, D41-D45, paper 29 , 1971.

18. Ibrahim, K. A., Mobbs, F. R. and Cole, B. N. " Theoretical Analysis of unsteady Gas- solid suspension flow in a shock tube " 4 th interntional conference for Mech. Power Eng., Cairo Univ., paper (V - 27)., 16 - 18 October 1982.

19. Gentry, R. A., Martin, R. E. and Daly, B. J. " An Eulerian differencing method for unsteady compressible flow problems ", J. Comp. Phys., Vol. 1, No. 1, PP. 87 - 118, July 1966.

20. Mobbs, F. R. Bowers, H. M. and Cole, B. N. " A theory for the high speed flow of gas-solids mixtures under conditions of equilibrium and constant fractional lag", Inst. of Mech. Engrs. and Inst. of Chem; Engrs. Joint Symposium on Two-phase Flow, Paper No. 8, 1969.

21. Outa, E., Tajima, K. and Morii, H. " Experiments and analyses on shock waves propagating through a gas-particle mixture", JSME, Vol.19, No. 130, P. 384, 1976.

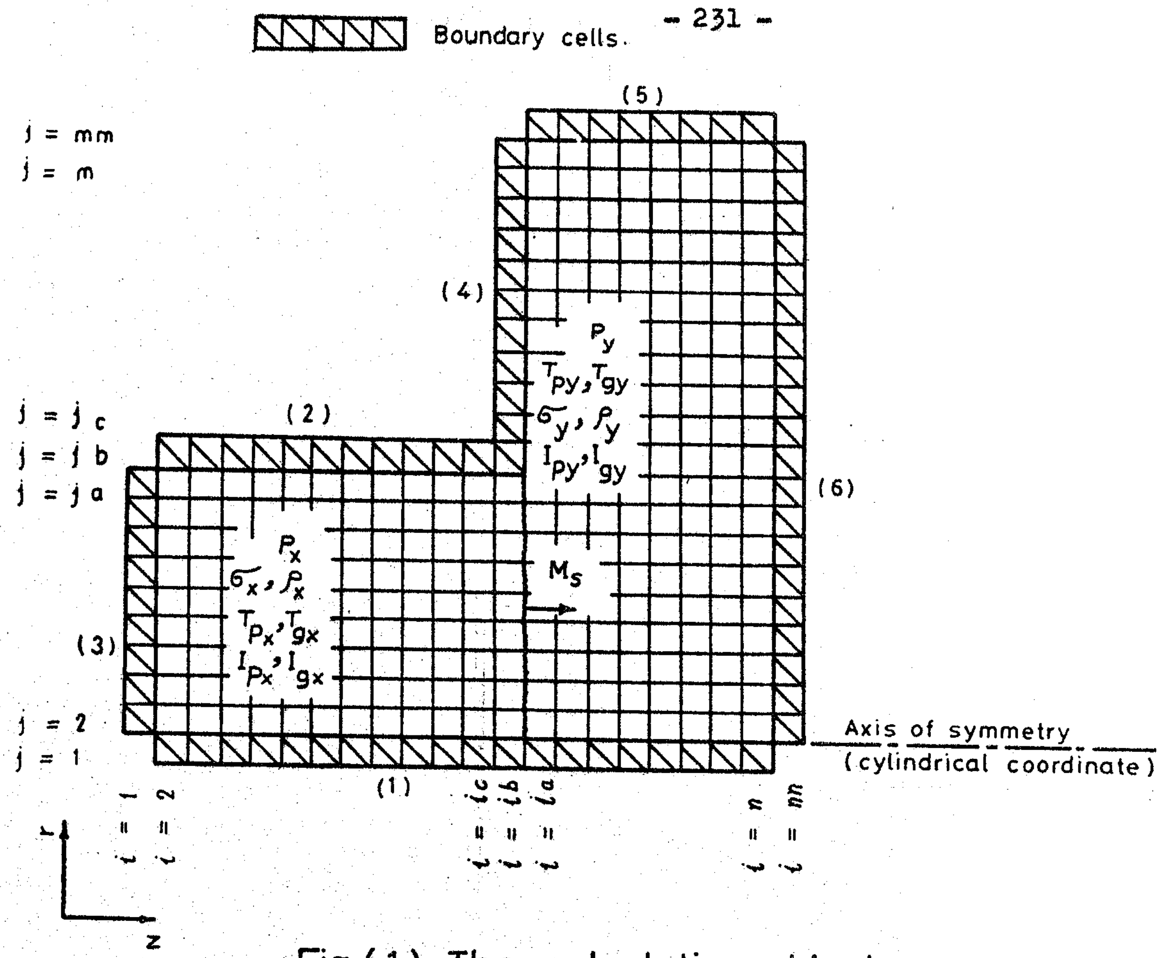

Fig.(1) The calculation Mesh.

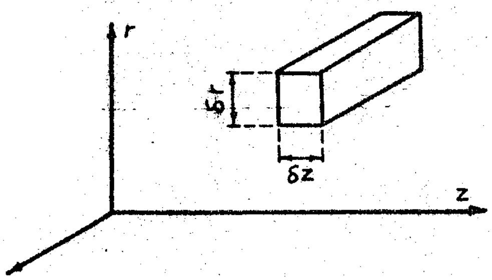

Fig.(2) Cartesian cell.

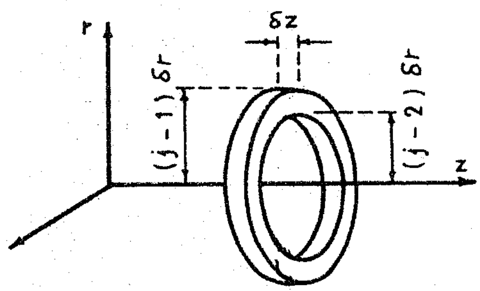

Fig.(3) Cylindrical cell.

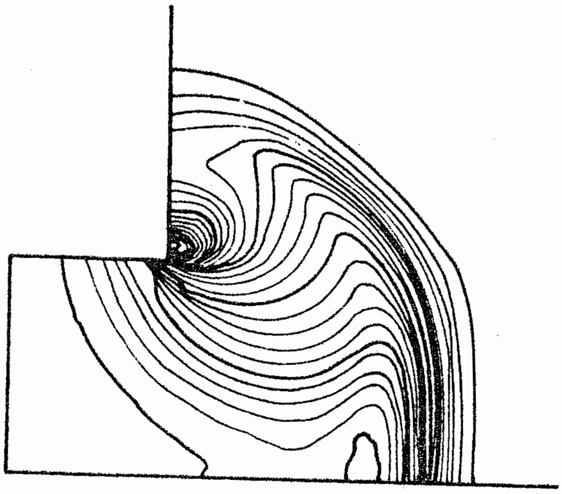

Fig.(4) Isobar plot at t = 100 μs
X = 0.0

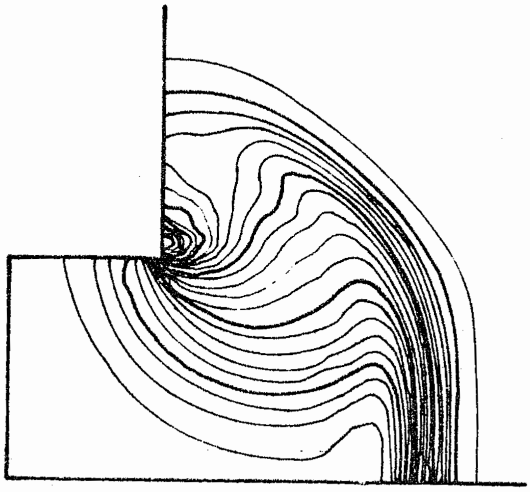

Fig.(5) Isobar plot at t = 100 μs
X = 1.0

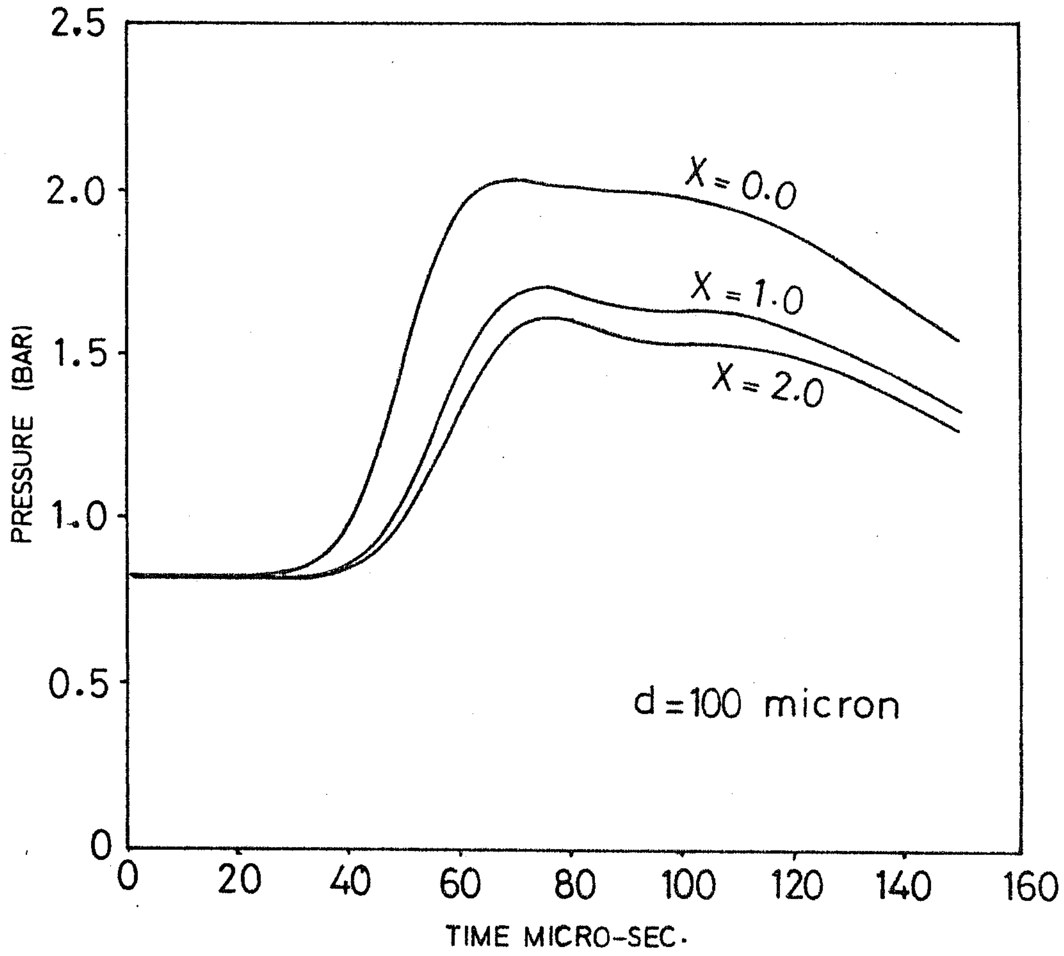

Fig.(6) Pressure history 25 mm
downstream of open end.

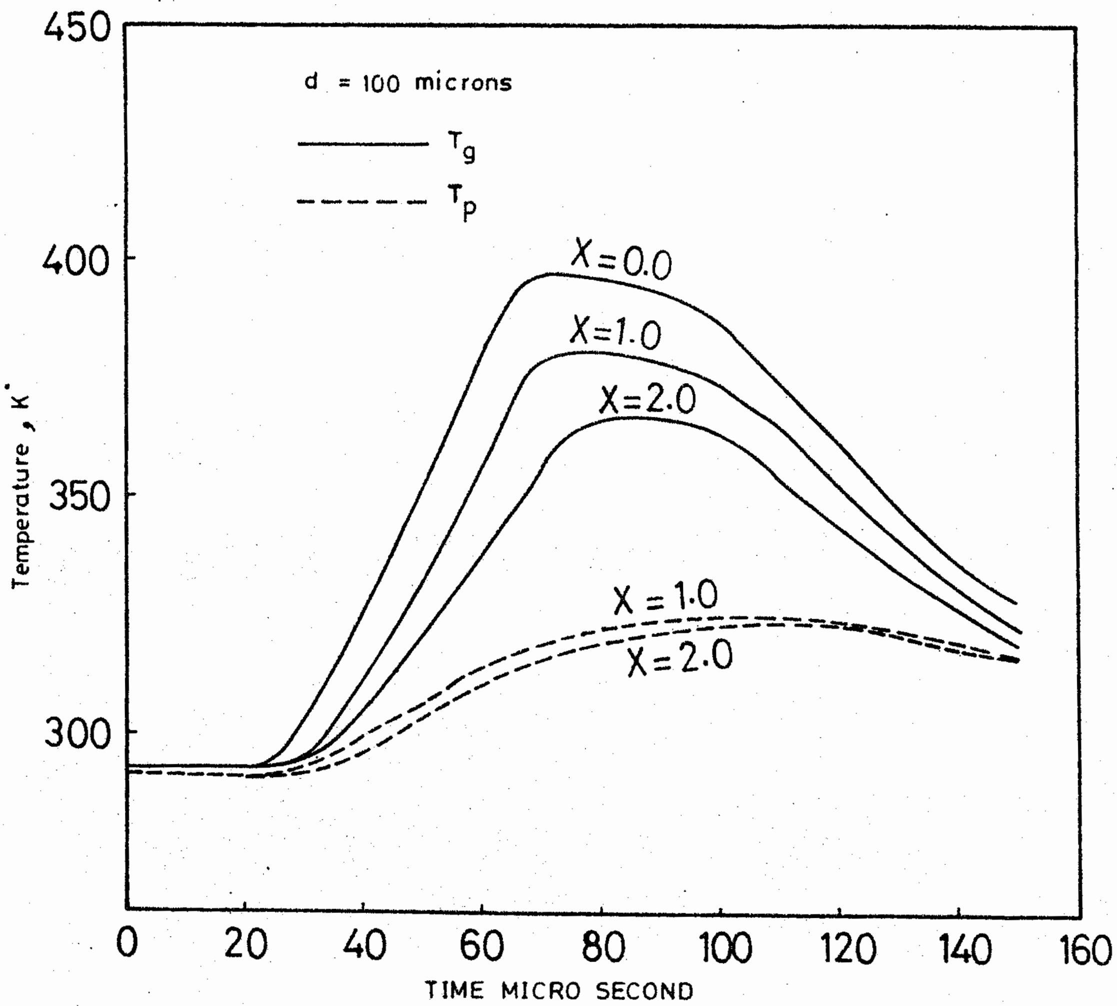

Fig (7) variation of gas and particle temperatures at 25 mm downstream of open end.

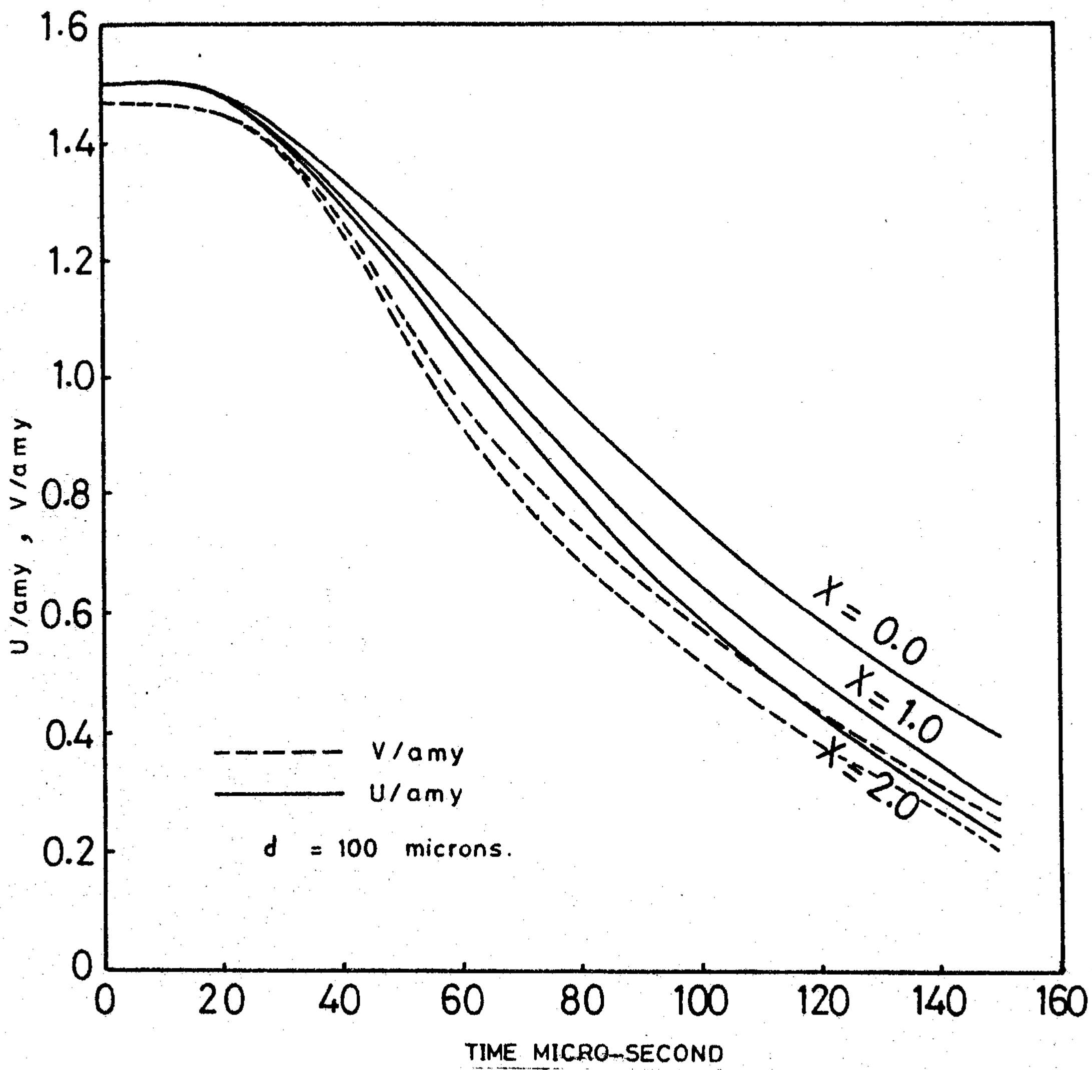

Fig.(8) variation of gas and particle velocities at 25 mm down stream of open end

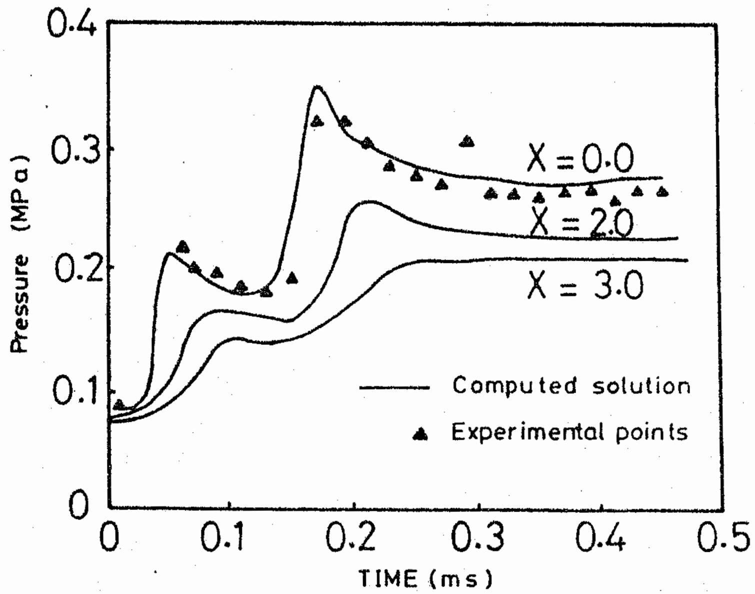

Fig.(9) Comparison of experimental results and computed pressure history.